MJMR, Vol. 34, No. 3, 2023, pages (132-145).

Open Access
ISSN:2682-4558

Research Article

Mitigating function of the dipeptidyl peptidase-4 inhibitor, sitagliptin, in silver nitrate experimentally induced pancreatic toxicity: the role of HIF-1α

Dalia Mohamed Ali[1], Sara M. Ahmed[2], Sara Mohamed Naguib Abdel Hafez[3], Nermeen N. Welson[4] and Walaa Yehia Abdelzaher[2]

[1] Department of Forensic Medicine and Clinical Toxicology, Faculty of Medicine, Minia University, Minia, Egypt.
[2] Department of Pharmacology, Faculty of Medicine, Minia University, Minia, Egypt.
[3] Department of Histology and Cell Biology, Faculty of Medicine, Minia University, Minia, Egypt
[4]Department of Forensic Medicine and Clinical Toxicology, Faculty of Medicine, Beni-Suef University, Beni Suef, Egypt.

DOI: 10.21608/MJMR.2023.225231.1482

Abstract

Background: Despite investigating silver toxicity in other organs, there is a dearth of literature about its effect on the pancreas. **Objectives:** The current study sought to determine if the antioxidant, anti-inflammatory, and anti-apoptotic properties of sitagliptin (Sit) could protect rats from pancreatic damage caused by silver nitrate ($AgNO_3$). **Materials and methods:** In both the presence and absence of $AgNO_3$, Sit was supplied. Four groups of 32 adult albino rats were formed as control, Sit (10mg/kg/ day p.o. for 28 days), $AgNO_3$ (20 mg Ag/kg/day in their drinking water for 28 days), and Sit/$AgNO_3$ (sit + $AgNO_3$ for 28 days) groups. Pancreatic enzymes and blood glucose level (BGL) were measured. In addition to pancreatic oxidative stress, inflammatory, and apoptotic indicators, pancreatic hypoxia-inducible factor 1-alpha (HIF-1α) was assessed. Pancreatic histopathological examination and antiinsulin immunohistochemical study were carried out. **Results**: $AgNO_3$ significantly elevated pancreatic enzymes, BGL, pancreatic oxidative stress, inflammatory, apoptotic biomarkers, and HIF-1α expression. Histopathological indicators of pancreatic toxicity and low antiinsulin expression were found. Sit substantially improved the histological image and mitigated the dispersed pancreatic enzymes, BGL, oxidative stress, inflammatory, and apoptotic indicators, as well as the expression of HIF-1 α. **Conclusion**: Sit abrogated AgNO3-induced pancreatic toxicity through modulating HIF-1α.

Keywords: sitagliptin; silver nitrate; pancreatic toxicity; HIF-1α.

Introduction

Silver nitrate ($AgNO_3$) is a common soluble silver salt. It has been proven to be an effective antiseptic for wound treatment for more than a century, and it is a better antibacterial agent than several other antibiotics, such as chlorhexidine and silver sulfadiazine. In skin wounds, $AgNO_3$ combines with proteins to form a resistant precipitate [1]. Its antibacterial action penetrates wounds very deeply, generating, in tissues, silver salts of silver albuminates and chloride. Calluses, warts, and ugly wound granulations can be removed as a result of its caustic and astringent actions. It has hemostatic qualities and could be helpful in simple surgery[2]. Water filtration is yet another very typical application for $AgNO_3$[3]

Ag compounds can get into the body by ingestion, inhalation, and skin contact. Ag is regarded as poisonous to both aquatic and terrestrial species, including humans[4,5]. Since $AgNO_3$ is corrosive and irritating, it

leads to cellular electrolytes like sodium and potassium to leak out. Target cells that are vulnerable to tissue regeneration are more susceptible to the cytotoxic effects of $AgNO_3$. It makes it possible for cells' proteins to break down, which prevents various types of cells from proliferating and differentiating [6]. Similar effects on uneven membrane boundaries and cell shrinkage were produced by $AgNO_3$ [7].

Reactive oxygen species (ROS), which are raised during oxidative stress, have been related to different biological and clinical diseases. According to reports, the toxicity of Ag ions destroys protein thiols and produces ROS [8]. Inflammatory cascades that cause inflammatory cell recruitment and tissue damage are mediated by reactive oxygen species (ROS). Oxidative stress is due to excessive ROS buildup in pathological circumstances like hypoxia. Pancreatic acinar cell destruction from severe acute pancreas-titis is caused by oxidative stress and ROS [9].

Hypoxia-inducible factor 1-alpha (HIF-1α), a component of a heterodimeric transcription factor, is regarded as the key transcriptional regulator of the body's response to hypoxia. Genes involved in glucose and iron metabolism, as well as cell survival and proliferation, are also activated by HIF-1α. NF-κB is required for the transcriptional regulation of HIF-1α abundance [10]. Most solid tumors investigated, including malignancies of the urinary, gastrointestinal, mammary, prostatic, and pancreatic systems, have been found to express HIF-1α significantly [11].

Type 2 diabetes is treated with the anti-diabetic drug sitagliptin (SIT). It functions to inhibit the enzyme dipeptidyl peptidase 4 (DPP-4) in a competitive manner. Plasma contains DPP-4, a membrane-bound aminopeptidase that controls inflammation and glucose homoeostasis [12]. This enzyme degrades the food-induced digestive hormones gastric inhibitory polypeptide (GIP) and glucagon-like peptide-1 (GLP-1). By preventing the degradation of GLP-1 and GIP, they are capable of boosting insulin secretion and inhibiting the secretion of glucagon by the pancreatic alpha cells. As a consequence, blood glucose levels (BGL) approach normal levels. Sit reduces DPP4 expression in the gut and decreases oxidative stress and inflammation in acute pancreatitis via the Nrf2-NF-B cascade [13].

Consequently, this experiment aimed to explore the possible mitigating effect of Sit against the pancreatic toxicity induced by $AgNO_3$, with a focus on the role of HIF-1α, as well as the probable mechanisms mediating its effect.

Materials and methods

Ethics

Rats were handled, given medications, and sacrificed in agreement with the NIH Guide for the Care and Use of Laboratory Animals, which contains recommendations for the management of experimental animals. The Faculty of Medicine at Minia University in Egypt's Institutional Ethical Committee gave its approval to the study. (Approval No. 8122021).

Chemicals and drugs

Sit was obtained from Multipharma, Egypt. AgNO3 was obtained from Sigma-Aldrich. Amylase and lipase colorimetrical kits were obtained from (Bio-Assay, USA). Reduced glutathione (GSH) was quantified colorime-trically using specific kits (Biodiagnostic, Egypt). Interleukin-6 (IL-6) and tumor necrosis factor-alpha (TNF-α) measured by ELISA kits (Elabscience, USA) (**Cat.No.:** E-EL-R0015; E-EL-R2856, respectively). Caspase-3 was evaluated by an ELISA kit (Cusabio, USA) (**Cat.No:** CSB-E08857r). Other chemicals were commercially obtained.

Animals and experimental design

The current study involved 32 adult male Wistar albino rats weighing between 210 and 230 g. The animals were acquired from the Animal Research Center in Giza, Egypt. Rats were kept in a suitable standard housing condition (3 rats per cage), fed chow, and given access to tap water. A week of acclimatization was left before starting the medications. Rats were randomly assigned into four groups, each with eight rats:

(1) Control group: rats received vehicles (carboxymethyl cellulose (CMC).

(2) Sit group: received sitagliptin (10 mg/kg/day) p.o. dissolved in CMC for 28 days [14].
(3) AgNO3 group: silver nitrate (20 mg Ag/kg/day) was added to their drinking water. Dosing volume was 4 ml/kg for 28 days [15, 16].
(4) Sit/AgNO3 group: received sitagliptin (10 mg/kg/day) and AgNO3 (20 mg/kg/day) for 28 days.
The doses and duration were selected according to our pilot study and the references mentioned previously.

Blood and tissue samples
At the end of the experiment, blood samples from each rat's tail were taken for measurement of fasting blood glucose level (BGL) using the ACCU-CHEK active blood glucose metre (Roche, Mannheim, Germany). Rats were then put to sleep using an IP injection of urethane (25% of a dose of 1.6 g/kg) before being put to death. From the rats' abdominal aorta, blood samples were taken. It was then centrifuged for 15 minutes at 4000g (Janetzki T30 centrifuge, Germany). The collected sera were then stored for use in biochemical analysis at -80°C. After being cleaned with saline, the pancreas was separated into two sections, with one stored at -80 degrees Celsius for biochemical study and the other placed in 10% formalin for histological evaluation.

Biochemical determination
Estimation of pancreatic enzymes
Serum amylase and lipase were estimated according to the manufacturer's recommend-dations (Bio-Assay, USA).

Estimation of pancreatic oxidative stress indicators
Pancreatic tissue was homogenized in potassium phosphate buffer 10 mM, pH (7.4). The ratio of tissue weight to homogenization buffer was 1:5. The homogenates were centrifuged at 4000 g for 10 minutes at 4°C. The resulting supernatant was used for the estimation of biochemical parameters.

Malondialdehyde (MDA) level, an index of lipid peroxidation, was measured according to the method described by Buege and Aust, 1978 [17].

Total nitrite/nitrate (NOx), the stable oxidation end products of nitric oxide, was used as an index of nitric oxide level and was detected by the reduction of nitrate into nitrite by the use of activated cadmium granules, followed by color formation with the Griess reagent in an acidic medium [18].

Estimation of inflammatory and apoptotic indicators
The levels of IL-6, TNF-α and caspase-3 in pancreatic tissue were measured using ELISA kits and the manufacturer's instructions.

Real-time reverse transcription poly-merase chain reaction (RT-PCR) of pancreatic HIF-1α gene expression
The gene expression of HIF-1α in pancreatic tissue was tested with the q RT-PCR technique. 100 mg of frozen tissue in total were weighed, and 1 ml of Trizol reagent was used to homogenise it (Invitrogen, USA). After 5–10 min incubation at 25°C, the homogenate was mixed with 0.2 ml of chloroform, rapidly shaken for 15 s, and then allowed to incubation for 3-min. The mixture was then centrifuged for 5 minutes at 10,000 ×g and 4°C. After getting the top layer of the mixture, 0.5 ml of isopropanol was applied. The samples were then centrifuged for 10 min. at 10,000 ×g and 4°C. The pellet was washed, suspended in 1 ml of 75% ethanol, and the supernatant was drained off. The residual pellet was centrifuged at 7000 ×g for 5 min at 4 °C. The majority of the ethanol was taken out, and the remainder was dried by air. A 50 µl volume of RNase-free water was added to a fully dried pellet before it was dissolved. Spectrometry was used to evaluate the isolated RNA's quantity and quality. By measuring the absorbance A260/A280, the concentrations and purity of RNA were ascertained. q RT-PCR for the measurement of mRNA expression was done on (Applied Biosyst 7500 fast, Techne (Cambridge) LTD., UK). On an Applied Biosyst 7500 Rapid, manufactured by Techne (Cambridge) Ltd. in the UK, q RT-PCR was used to measure the expression of mRNA quantita-tively. Following the manufacturer's guidelines, RNA extract was reverse transcribed and q RT-PCR was carried out

(Thermo Scientific one-step kits, including ROX Vial, Code No. AB-4104/A). All primers were purchased from Eurofins Genomics, Europe. On an Applied Biosyst 7500 Rapid, manufactured by Techne (Cambridge) LTD. in the UK, q RT-PCR was used to measure the expression of mRNA quantitatively. Following the manufacturer's guidelines, RNA extract was reverse transcribed, and q RT-PCR was carried out (Thermo Scientific one-step kits, including ROX Vial, Code No. AB-4104/A). We bought all of our primers from Eurofins Genomics in Europe. Every target gene's level of expression was normalized in relation to the level of B-actin mRNA expression. The primer sets used were:
HIF-1α forward: 5′-TCC ATTATG AGG CTG ACC ATC-3′ and reverse: 5′-CCATCC TCA GAA AGC ACC ATA-3′
B-actin forward: 5′- CCC GCG AGT ACA ACC TTC T-3′ and reverse: 5′- CGT CAT CCATGG CGA ACT-3′

The relative expression of the genes was calculated using the formula used by VanGuilder et al., 2008 [19], 2 (−ΔΔCt). They were scaled in comparison to controls, with the value of the control samples set to one. For all experimental samples, the data was thus graphically represented as relative expression vs. control.

Histopathology and immunohistochemical study

Small samples of pancreatic tail tissue were quickly preserved in 10% buffered formalin before being examined under a light microscope.
Tissues were processed for 1) hematoxylin and eosin (H&E)[20], 2) periodic acid Schiff (PAS)[21], and 3) avidin-biotin peroxidase immunohistochemistry staining for estimation of anti-insulin antibodies. The manufacturer's instructions were followed using rabbit monoclonal anti-insulin antibodies (Abcam, USA, ab181547)[22] at a dilution of 1:500, then hematoxylin counter-staining according to the manufacturer's guidelines [23]. Positive tissue control: slides of control rat pancreatic tissue. Negative control: Slides of control pancreatic tissue were subjected to the same previous steps, but without using the primary antibody.

Image capture

Light microscopy examination of the slices was done (Olympus, Japan). Using a high-resolution colour digital camera (Olympus, Japan) customized for the microscope and linked to the computer, photomicrographs were digitally recorded.

Morphometrical study

All parameters were assessed in 10 non-overlapping fields within each slide (three sections per animal), using power × 400 [24].
Quantitative data were collected for three parameters:
1- Measuring the mean area fraction of anti-insulin immunoreactivity using Image J 22 software (open-source Java image processing program) was used. The area fraction was calculated using a standard measuring frame that was linked to the monitor screen. The areas containing positive immunoreaction tissues were measured [22].
2- Measuring the mean area fraction of PAS using Image J 22
3- Mean diameter of islets of Langerhans (µm). The average islet core diameter was measured, excluding the extension areas.

Statistical Analysis

A one-way ANOVA followed by Tukey's multiple comparison test was used. Results were displayed as means ± SEM. GraphPad Prism software (version 5) was used for analysis. A p-value less than 0.05 was set for significance.

Results

Effect of Sit on pancreatic enzymes in $AgNO_3$-induced pancreatic toxicity in rats

In Figure 1, the $AgNO_3$ group displayed significant elevations in serum lipase and amylase enzymes relative to the control and Sit groups. When compared to the $AgNO_3$ group, the Sit/$AgNO_3$ group showed significant decreases in serum lipase and amylase enzymes.

Effect of Sit on oxidative stress indicators in $AgNO_3$ caused pancreatic toxicity in rats

In comparison to the control and Sit groups, the $AgNO_3$ group had significant increases in pancreatic MDA and NOx and a significant decrease in pancreatic GSH. However, when

compared to the $AgNO_3$ group, the Sit/$AgNO_3$ treated group showed a significant normalization in oxidative stress indicators (Table 1).

Table 1: Effect of Sit on oxidative stress parameters in $AgNO_3$ induced pancreatic toxicity in rats

Groups	Pancreatic MDA (nmol/g tissue)	Pancreatic GSH (nmol/g tissue)	Pancreatic NOx (nmol/g tissue)
Control	91.05 ± 2.68	73.62 ± 2.40	30.80 ± 1.54
Sit	91.97 ± 3.33	73.33 ± 2.93	31.82 ± 2.05
$AgNO_3$	191.00 ± 4.88^{ab}	40.12 ± 1.24^{ab}	62.65 ± 2.16^{ab}
Sit/$AgNO_3$	102.20 ± 5.02^{c}	66.07 ± 1.92^{c}	37.15 ± 1.81^{c}

Results represent the mean ± SEM (8 rats/group). [a] Significant ($P < 0.05$) difference from the control group. [b] Significant ($P< 0.05$) difference from the Sit group. [c]Significant ($P<0.05$) difference from AgNO3. [Sit: sitagliptin; AgNO3: Silver nitrate; MDA = malondialdehyde; GSH = reduced glutathione and NOx = total nitrite/nitrate].

Effect of Sit on BGL in $AgNO_3$ induced pancreatic toxicity in rats

In Table 2, the $AgNO_3$ group displayed a significant elevation in BGL when compared to the control and Sit groups. However, the Sit/$AgNO_3$-treated group displayed a significant decrease in BGL when compared to the $AgNO_3$ group.

Table 2: Effect of Sit on liver enzymes and BGL in $AgNO_3$ induced pancreatic toxicity in rats

Groups	BGL (mg/dl)
Control	82.88± 3.33
Sit	76.25 ± 2.96
$AgNO_3$	229.80± 19.34^{ab}
Sit/$AgNO_3$	114.80± 4.169^{c}

Results represent the mean ± SEM (8 rats/group). [a] Significant ($P < 0.05$) difference from the control group. [b] Significant ($P< 0.05$) difference from the Sit group. [c]Significant ($P<0.05$) difference from $AgNO_3$. [Sit: sitagliptin; AgNO3: Silver nitrate; BGL: blood glucose level].

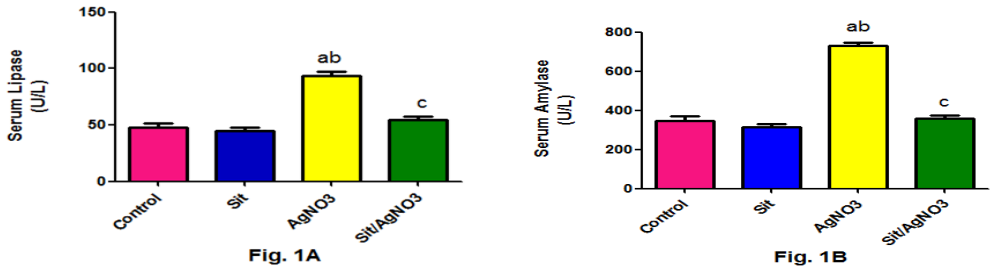

Figure 1: Effect of Sit on serum pancreatic enzymes in AgNO3 induced pancreatic toxicity in rats. Results represent the mean ± SEM (8 rats/group). [a] Significant ($P < 0.05$) difference from the control group. [b] Significant ($P< 0.05$) difference from the Sit group. [c]Significant ($P<0.05$) difference from $AgNO_3$. [Sit: sitagliptin; $AgNO_3$: Silver nitrate].

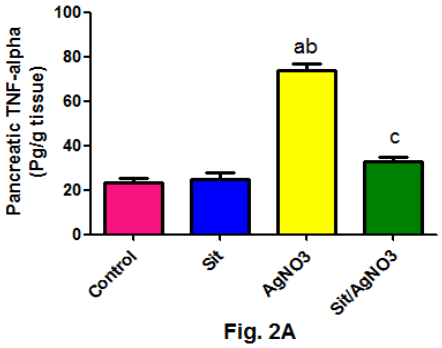

Fig. 2A

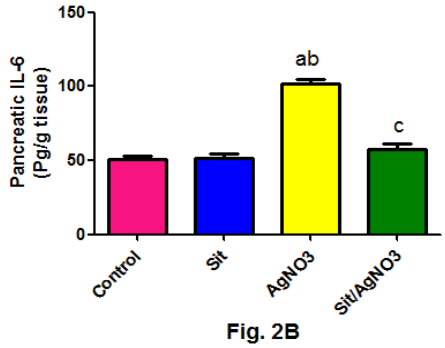

Fig. 2B

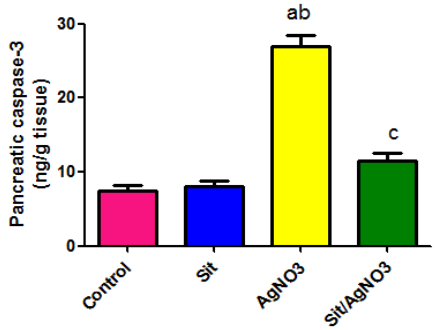

Fig. 2C

Figure 2: Effect of Sit on pancreatic inflammatory and apoptotic markers in AgNO3 induced pancreatic toxicity. Results represent the mean ± SEM (8 rats/group). [a] Significant ($P < 0.05$) difference from the control group. [b] Significant ($P< 0.05$) difference from the Sit group. [c]Significant ($P<0.05$) difference from $AgNO_3$. [Sit: sitagliptin; $AgNO_3$: Silver nitrate; TNF-α: tumor necrosis factor-alpha; IL-6: Interleukin-6].

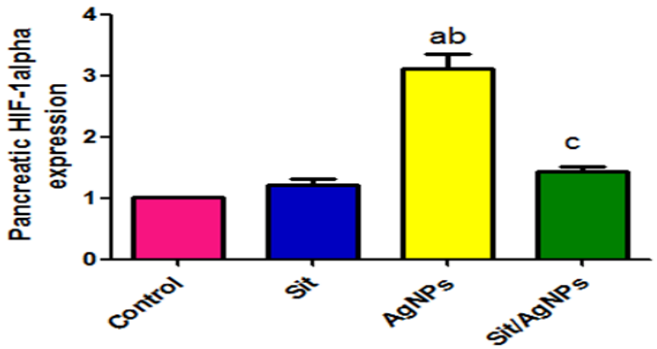

Fig 3

Figure 3: Effect of Sit on pancreatic HIF-1 α expression in $AgNO_3$ induced pancreatic toxicity in rats. Results represent the mean ± SEM (8 rats/group). [a] Significant ($P < 0.05$) difference from the control group. [b]Significant ($P< 0.05$) difference from the Sit group. [c]Significant ($P<0.05$) difference from $AgNO_3$. [Sit: sitagliptin; $AgNO_3$: Silver nitrate; HIF-1 α**:** hypoxia-inducible factor 1-alpha].

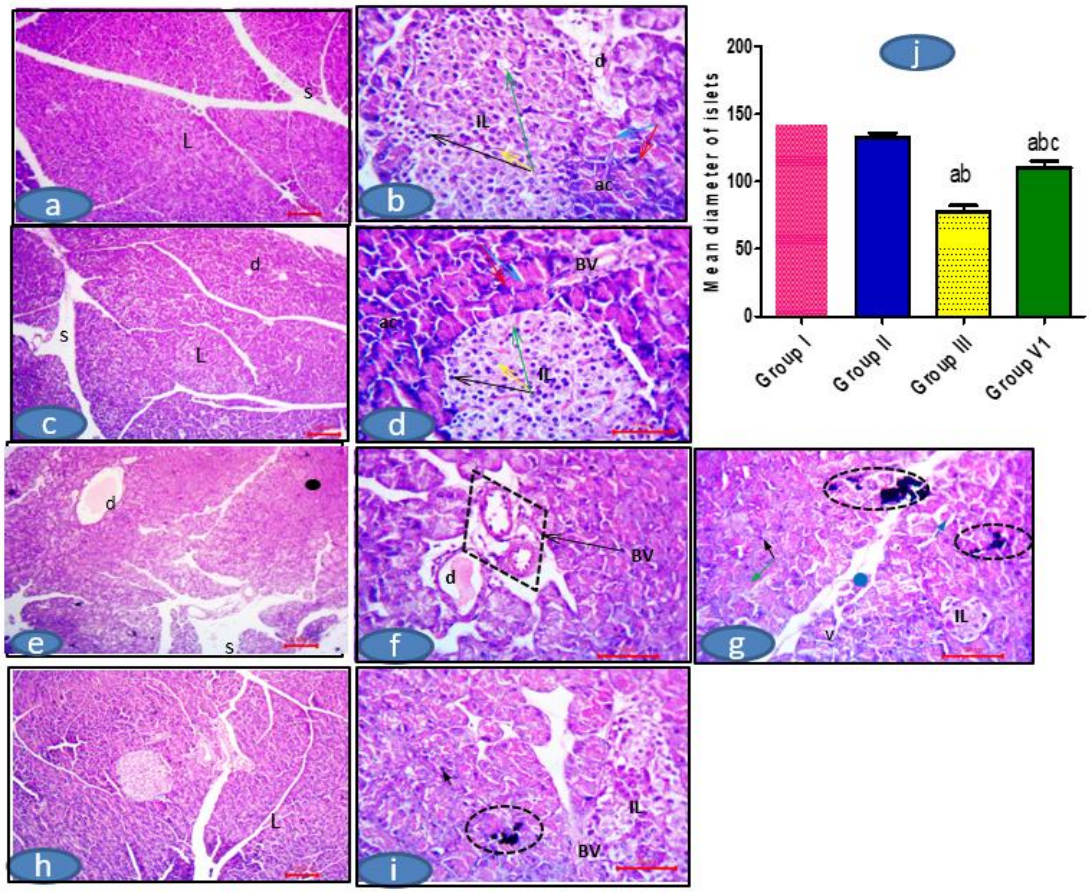

Fig 4: Representative photomicrographs of rat pancreatic tissue. a–b) control group & c-d) Sit group showing the same morphological picture. a&c) Showing the pancreatic lobules (L). The interlobular septum (S) separates these lobules (L). b&d) showing pancreatic lobules forms of exocrine portion (ac); composed of closely packed secretory acini and the pale-stained area; endocrine portion (islets of Langerhans (IL). Islets of Langerhans consist of endocrine cells arranged into cords that have both pale (yellow arrow) and dark (black arrows) stained cells. Blood sinusoids (green arrows) are seen between these cells. Pancreatic acini formed of pyramidal-shaped acini. Acinar cells display intense basal basophilia (red arrows) and apical acidophilia (blue arrow). e-g) $AgNO_3$ group showing e) distorted lobular architecture, wide inter-lobular septa and dilated intralobular duct retained secretion (d). f) Dilated interlobular blood vessels (BV). g) showing Islet's of Langerhans cells with reduced its cellularity (IL). Some distorted acini appear with small dense nucleus (black arrow). Others lost their basal basophilia (green arrow). The circles showing large melanomacrophages. h-i) Sit/AgNO3 group showing h) More or less normal pancreatic lobules (L). i) Less notable dilated blood vessels (BV) are observed. Islet of Langerhans (gl) showing apparent increase in its cellularity. Most Langerhans cells appear with vesicular nuclei. Almost all acini retain their apical acidophila and basal basophilia. The circle showing small melanomacrophage. H&E, scale bar: a, c,e,h X 200 µm; b, d, f, g , i X 50 µm.

j) Histogram showing the mean diameter of islets of Langerhans (mm) in all studied groups. Results represent the mean ± SEM (8 rats /group). [a] Significant ($P < 0.05$) difference from the control group. [b]Significant ($P< 0.05$) difference from the Sit group. [c]Significant ($P<0.05$) difference from $AgNO_3$. [Sit: sitagliptin; AgNO3: Silver nitrate].

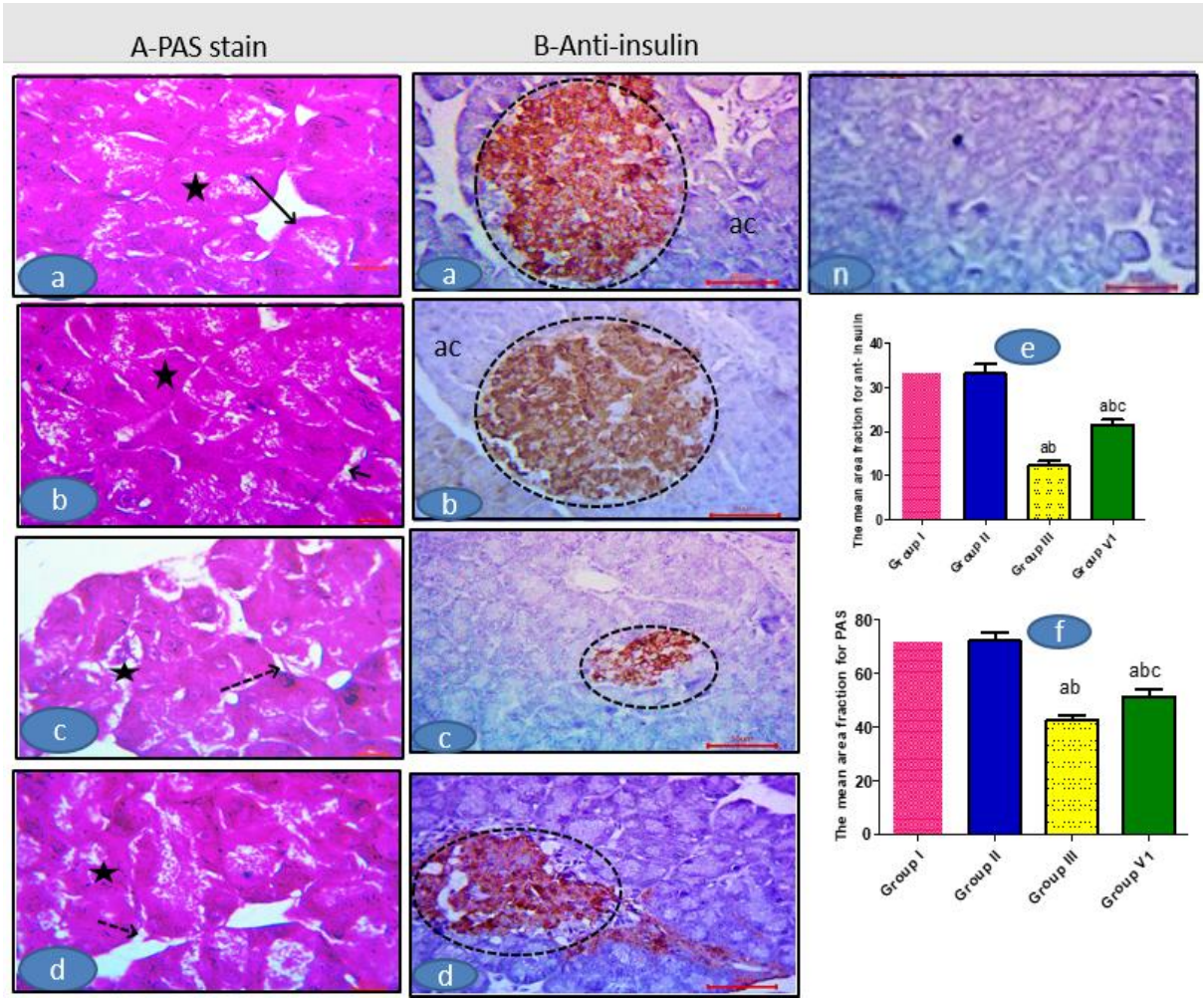

Fig 5: Representative photomicrographs of rat pancreatic tissue of PAS & Anti insulin immunostaining. PAS staining showing a&b) control and Sit groups respectively showing the same positive PAS reaction in the BMs of pancreatic acini (black arrow). Notice the staining of the cytoplasm of these acini (star). C) AgNO3 group showing interruption and separation of the BMs at many sites (dash black arrow). Some acinar cells (star) show less PAS reaction (star). d) Sit/AgNO3 group showing less interruption and separation of the BMs at few sites (dash black arrow). Most acinar (star) cells show more PAS reaction (star). PAS, scale bar × 50 µm
Anti-insulin staining showing n) Negative control for anti-insulin. a&b) control and Sit groups respectively displaying positive cytoplasmic β-cells staining (circles) occupying most of the islet's cells with negative reaction in the acini (stars). c) $AgNO_3$ group showing few positive immunostained β cells in apparently shrunken islet. d) Sit/$AgNO_3$ group showing positive reaction in apparent more numerous β cells (circle. Notice the insulin positive cells lining acinar cells (rectangle) connecting to the islets. Immunohistochemistry, counterstained with H, scale bar × 50 µm. e) Histogram showing the mean area fraction for antiinsulin in all studied groups. Results represent the mean ± SEM (8 rats /group). [a] Significant ($P < 0.05$) difference from the control group. [b]Significant ($P< 0.05$) difference from the Sit group. [c]Significant ($P<0.05$) difference from $AgNO_3$. [Sit: sitagliptin; $AgNO_3$: Silver nitrate]. f) Histogram showing the mean area fraction for PAS in all studied groups. Results represent the mean ± SEM (8 rats /group). [a] Significant ($P < 0.05$) difference from the control group. [b] Significant ($P< 0.05$) difference from the Sit group. [c]Significant ($P<0.05$) difference from $AgNO_3$. [Sit: sitagliptin; AgNO3: Silver nitrate].

Effect of Sit on inflammatory and apoptotic indicators in $AgNO_3$ caused pancreatic toxicity in rats

Figure 2 depicted significant increases in pancreatic TNF-α, IL-6 levels, as well as caspase-3 activity, in the $AgNO_3$ group compared to the control and Sit groups. In comparison to the $AgNO_3$ group, the Sit/$AgNO_3$ group had significantly lower pancreatic TNF-α, IL-6 levels, and caspase-3 activity.

Effect of Sit on gene expression of HIF-1α in $AgNO_3$ caused pancreatic toxicity in rats

The $AgNO_3$ group had significantly increased HIF-1α expression relative to the control and Sit groups, while the Sit/$AgNO_3$ group had significantly decreased HIF-1α expression relative to the $AgNO_3$ group (Figure 3).

H&E results

The control and Sit groups showed the same morphological picture. The pancreatic lobules were composed of both endocrine (Islets of Langerhans) and exocrine (pancreatic acini) parts. The interlobular septum separated these lobules and contained blood vessels and ducts. Regarding the endocrine portion, the islets of Langerhans (pale-stained areas among the exocrine portion) consisted of endocrine cells arranged into cords that have both pale and dark-stained cells. Blood sinusoids were noticed among the cells. The exocrine part was formed of closely packed secretory acini.

Pyramidal-shaped cells made up pancreatic acini. Acinar cells displayed intense basal basophilia and apical acidophilia. In contrast, the $AgNO_3$ group showed distorted lobular architecture, widening interlobular septa, and dilated intralobular ducts that retained secretion. Dilated interlobular blood vessels were also noticed. Islets of Langerhans cells were seen with reduced cellularity. Some distorted acini appeared with small, dense nuclei. Others lost their basal basophilia. On examining wide fields of sections, large melanomacrophages (aggregates of highly pigmented phagocytes) were frequently seen. Furthermore, the Sit/$AgNO_3$ group showed more or less normal pancreatic lobules. Dilated blood vessels were found to be less noticeable. The Islet of Langerhans displayed an apparent increase in its cellularity. Most Langerhans cells appeared to have vesicular nuclei. Almost all acini retained their apical acidophila and basal basophilia. Small melanomacrophages were also observed (Figure 4).

PAS staining in the control and Sit groups revealed the same positive PAS reaction in the basement membranes (BMs) of pancreatic acini and in the cytoplasm of these acini (star). The $AgNO_3$ group displayed interruption and separation of the BMs at many sites. Some acinar cells displayed less reaction. In contrast, the Sit/$AgNO_3$ group showed less interruption and separation of these BMs at a few sites, and most acinar cells showed more PAS reaction if compared with the $AgNO_3$ group (Figure 5A).

Anti-insulin immunostaining in the control and Sit groups showed positive cytoplasmic cell staining, occupying the majority of the islet cells, with a negative reaction in the acinar cells in this study. Meanwhile, the AgNO3 group showed a few positive immunostained β cells in apparently shrunken islets. In contrast, the Sit/$AgNO_3$ group exhibited a positive reaction in the apparent more numerous β cells, and it was interesting to notice the insulin-positive cells lining the acinar cells connecting to these islets (Figure 5B).

Quantitative morphometric findings

There were highly significant differences in the mean diameter of islets, the mean area fraction of PAS, and anti-insulin expressions in the $AgNO_3$ group relative to the control and Sit groups. However, the Sit/AgNO3 group revealed a highly significant difference in all these parameters relative to the AgNO3 group (Figure 4 & 5).

Discussion

Silver ions (Ag+) dissociate from various salts and silver particles [25]. Since silver has not yet been recognised as a trace metal, it appears that it is not necessary for human physiology [3]. Consequently, it is thought that exposure to silver is undesirable.

This study aimed to explore $AgNO_3$-induced pancreatic toxicity and the possible protective effect of Sit against this toxicity.

The current experiment proved the pancreatic toxicity related to the soluble silver salt, AgNO3, through the elevated pancreatic markers. Despite investigating silver toxicity in other organs, there is a dearth of literature about its effect on the pancreas. An earlier study by Tiwari et al., 2021 [26] examined the effect of prenatal exposure to silver nanoparticles (AgNPs) in mice and proved pancreatic and renal damage later in life. As a result, Ag+ had an effect on the pancreas, causing an increase in pancreatic enzymes. They are good indicators for pancreatic injury diagnosis. The development of hydrolytic enzymes following pancreatic damage that hydrolyze phospholipids to arachidonic acid and lysophospholipids with a cytotoxic effect may be associated with elevated levels of pancreatic enzymes. Additionally, there is necrosis and deformed acinar cells, which cause the pancreatic enzymes, primarily amylase and lipase, to rise [27]. It is remarkable that Sit markedly increased the serum levels of lipase and amylase.

The present work showed marked pancreatic oxidative injury with $AgNO_3$ in the form of elevated pancreatic MDA and NOx with decreased GSH. The toxicity of Ag+ destroys protein thiols and produces ROS [8]. Oxidative stress is due to excessive ROS buildup in pathological circumstances like hypoxia. Due to the extremely low expression of anti-oxidant enzymes in pancreatic islet cells, the pancreatic tissue is more vulnerable to oxidative stress than other tissues. In pancreatic injury, oxygen-free radicals are produced as a result of the damage to acinar cells. The pancreas and liver are connected anatomically, physiologically, and hemodynamically. The liver becomes afflicted as a result of ROS from pancreatic injury reaching it through the blood circulation, which causes a reduction in the liver's capacity to remove free radicals and an increment in the body's response to oxidative stress[28]. Our findings are consistent with those of Gueroui and Kechrid, 2016 [16], who found that $AgNO_3$ is a major cause of oxidative injury in the rat brain, contributing to the development of cytotoxicity. The present result showed that Sit-treated rats had significantly improved oxidative stress parameters, which coincides with earlier studies reporting the antioxidant effect of Sit in different tissues (brain [29], testes[30], and uterus[31]). Kong and his coworkers, 2021[32] also support current results, as they reported that Sit reduced oxidative damage and marked autophagy associated with severe acute lung injury on top of acute pancreatitis in mice.

BGL was significantly higher in the $AgNO_3$ group, indicating that Ag+ has a significant effect on glucose homeostasis. This clearly demonstrates that exposure to $AgNO_3$ causes harm to the pancreas, which disrupts the organ's normal endocrine function[26]. Because of the strong interaction between the exocrine and endocrine sections of the pancreas [33], the endocrine function with $AgNO_3$ was also degraded, as evidenced by the following identified changes: the islets of Langerhans appeared with less cellularity, which was confirmed by the immune-histochemical study. Sit significantly improved BGL via boosting insulin production and decreasing glucagon secretion by the pancreatic alpha cells by preventing the hydrolysis of GLP-1 and GIP. As a consequence, BGL got closer to average [13].

In the present experiment, $AgNO_3$ significantly elevated pancreatic TNF-α and IL-6 levels as markers of inflammation, indicating pancreatic injury. These findings are consistent with previous research indicating that pancreatic injury is associated with inflammatory cytokine release [2]. TNF-α is one of the key mediators of inflammation. It first appeared during the early stages of the disease along with an increase in the pancreatic endothelial cells' permeability. On the other hand, it promotes the creation and release of other cytokines that start the generation of lymphocytes and neutrophils. Additionally, IL-6 plays a role in the body's immunological response because T-cells generate it, and this pro-inflammatory cytokine stimulates the immune system when an infection, injury, or tissue damage results in inflammation. Numerous investigations

showed a strong connection between pancreatic damage and the level of IL-6[2,28,34]

Sit's anti-inflammatory ability is evident in our findings, as Sit significantly reduced TNF-α, IL-6 levels. This supported by Abdelzaher and her colleges, 2020 [30] who reported that Sit was protective against testicular injury mostly by its anti-oxidative stress, and anti-inflammatory roles. Additionally, Wadie et al**.,** 2022 [35] noticed that Sit potentiated the effect of insulin in improving TNF-α, IL-6 levels in cardiac dysfunction in diabetic rats.

The cysteine-aspartic acid protease (caspase-cascade) family includes caspase-3 [36]. The execution phase of cell apoptosis is primarily characterized by the sequential activation of caspases by a variety of triggers [37]. The current study found a significant increase in caspase-3 in the $AgNO_3$ group. $AgNO_3$ induced large frequencies of cellular apoptosis as a result of all the silver metal complexes [38]. Sit improved the apoptotic marker caspase-3 significantly as Sit has an anti-apoptotic action, which has been confirmed by various studies [30, 31, 35].

Hypoxia-inducible factor 1-alpha (HIF-1α), a component of a heterodimeric transcription factor, is regarded as the key transcriptional regulator of the body's response to hypoxia. Genes involved in glucose and iron metabolism, as well as cell survival and proliferation, are also activated by HIF-1α [10]. The present study revealed that $AgNO_3$ significantly increased HIF-1α expression. Eom et al., 2013 [39] found that AgNPs increased the expression of HIF-1α due to the oxidative stress caused by AgNPs. As the same, $AgNO_3$ increased oxidative stress, followed by increased HIF-1α expression through attenuating its protein accumulation and downstream expression. In addition to the development of oxidative stress, the increase in HIF-1α expression was linked to the induction of apoptosis and inflammation. This supports the multiple publications that indicated a substantial correlation between the rise in oxidative stress, apoptosis, and inflammatory markers and the boost in HIF-1α in different organs [30, 40, 41].

The von Hippel-Lindau protein, that is essential for degradation of HIF-1α, became inactive in the mice with impairment of pancreatic beta-cell function [42]. HIF-1α is quickly destroyed under normoxic circumstances by the ubiquitin-dependent proteasome 26S route following hydroxy-lation and ubiquitination. Contrarily, it is generally accepted that HIF-1α accumulates under hypoxic circumstances as a result of hydroxylation inhibition [43].

Running in the same stream, in the present results, Sit repressed HIF-1α expression, which accompanied the decrease in oxidative injury, apoptosis, and inflammatory markers. That action emphasised the function of HIF-1α suppression in preventing $AgNO_3$ injury to the pancreas. This coincides with Abdelzaher et al., 2020 [30] who stated that Sit decreased HIF-1α expression in the testicular ischemia reperfusion model in rats.

The current biochemical markers were confirmed by the histological results. As various morphological changes were detected in pancreatic tissue, they affected both the endocrine and exocrine portions. The pancreatic acini were distorted and appeared to have small, dense nucleoli. Many acini lost their basal basophilia. Melano-macrophages were frequently observed among the sections in the $AgNO_3$ group in pancreatic tissue. Several lines of evidence suggested that melanomacrophages centres were aggregates of highly pigmented phagocytes settled mainly in the kidney and spleen, and occasionally the liver of many vertebrates and they demonstrated that these cells resembled the mammalian germinal centre architecturally, which led to the theory that they were crucial to the humoral adaptive immune reaction [44, 45].

Histologically, all the previously mentioned pathological changes were ameliorated in Sit-treated rats. Surprisingly, the current study found insulin-secreting cells in pancreatic acini that are nearly as numerous as the "apparent normal islets" of Langerhans. This may suggest the role of pancreatic cells in the regeneration of B cells. According to Okuno et al., 2007 [46], pancreatic acinar cells may

serve as a source of autologous transplantable insulin-secreting cells for the treatment of type 1 diabetes because they were shown to be capable of trans-differentiating into insulin-secreting cells in animals with diabetes.

Conclusion

Through the control of HIF-1α, sit has powerful ameliorative benefits against the pancreatic toxic impact of $AgNO_3$. These effects include a reduction in oxidative stress, inflammation, and apoptosis. We believe that our findings will shed light on future research and have therapeutic implications for its application to lessen the aforementioned pancreatic toxicity in those receiving AgNO3.

Conflict of interest

The authors declare that they have no known competing financial interests or personal relationships that could have appeared to influence the work reported in this paper.

Authorship contribution statement

DMA, SMA, and WYA Designed and performed the experiment, data analysis, supervision and writing the manuscript. SMNAH Performed histological and immunohistochemical examinations. NNW Cooperated in writing, editing, and revising the manuscript. All authors revised and approved the manuscript.

DMA: Conceptualization, Methodology, Preparation. SMA: Resources, Writing – original draft. SMNAH: Methodology, investigations. NNW: Writing – review & editing. WYA: Conceptualization, Supervision.

Funding sources

This research did not receive any specific grant from funding agencies in the public, commercial, or not-for-profit sectors.

References

2- Lansdown AB. A guide to the properties and uses of silver dressings in wound care. Prof Nurse. 2005;20(5):41-43.
3- Hadrup N, Lam HR. Oral toxicity of silver ions, silver nanoparticles and colloidal silver--a review. Regul Toxicol Pharmacol. 2014;68(1):1-7. doi:10.1016/j.yrtph.2013.11.002
4- Lansdown AB. Silver in health care: antimicrobial effects and safety in use. Curr Probl Dermatol. 2006;33:17-34. doi:10.1159/000093928.
5- Kwon JT, Minai-Tehrani A, Hwang SK, et al. Acute pulmonary toxicity and body distribution of inhaled metallic silver nanoparticles. Toxicol Res. 2012;28(1): 25-31. doi:10.5487/TR.2012.28.1.025
6- Roh JY, Eom HJ, Choi J. Involvement of Caenohabditis elegans MAPK Signaling Pathways in Oxidative Stress Response Induced by Silver Nanoparticles Exposure. Toxicol Res. 2012; 28(1):19-24. doi:10.5487/TR.2012.28.1.019
7- Hidalgo E, Domínguez C. Study of cytotoxicity mechanisms of silver nitrate in human dermal fibroblasts. Toxicol Lett.1998;98(3):169-179. doi:10.1016/s0378-4274(98)00114-3.
8- Hussain SM, Javorina AK, Schrand AM, Duhart HM, Ali SF, Schlager JJ. The interaction of manganese nanoparticles with PC-12 cells induces dopamine depletion. Toxicol Sci. 2006;92(2):456-463. doi:10.1093/toxsci/kfl020
9- Miyayama T, Arai Y, Suzuki N, Hirano S. Mitochondrial electron transport is inhibited by the disappearance of metallothionein in human bronchial epithelial cells following exposure to silver nitrate. Toxicology. 2013;305:20-29. doi:10.1016/j.tox.2013.01.004
10- Kong L, Deng J, Zhou X, et al. Sitagliptin activates the p62–Keap1–Nrf2 signalling pathway to alleviate oxidative stress and excessive autophagy in severe acute pancreatitis-related acute lung injury. Cell Death Dis. 2021; 12:928. doi:10.1038/s41419-021-04227-0.
11- van Uden P, Kenneth NS, Rocha S. Regulation of hypoxia-inducible factor-1alpha by NF-kappaB. Biochem J. 2008;412(3):477-484. doi:10.1042/BJ20080476.
12- Ezzeddini R, Taghikhani M, Somi MH, Samadi N, Rasaee MJ. Clinical Importance of FASN in Relation to HIF-1α and SREBP-1c in Gastric Adenocarcinoma. Life Sci. 2019; 224: 169–76.doi: 10.1016/j.lfs.2019.03. 056
13- Bassendine MF, Bridge SH, McCaughan GW, Gorrell MD. COVID-19 and comorbidities: A role for dipeptidyl peptidase 4 (DPP4) in disease

severity?. J Diabetes. 2020;12(9):649-658. doi:10.1111/1753-0407.13052
14- Zhou X, Wang W, Wang C, et al., DPP4 Inhibitor Attenuates Severe Acute Pancreatitis-Associated Intestinal Inflammation via Nrf2 Signaling. Oxid Med Cell Longev. 2019; 2019:6181754. Published 2019 Nov 15. doi:10.1155/2019/6181754.
15- Shawky L M, Morsi A A, El Bana E, Hanafy S M. The Biological Impacts of Sitagliptin on the Pancreas of a Rat Model of Type 2 Diabetes Mellitus: Drug Interactions with Metformin. Biology. 2020; 9: 6. doi:10.3390/biology9010006
16- Charehsaz M, Hougaard K S, Sipahi H, et al. Effects of developmental exposure to silver in ionic and nanoparticle form: A study in rats. DARU J Pharm Sci. 2016; 24:24. DOI 10.1186/s40199-016-0162-9
17- Gueroui M and Kechrid Z. Evaluation of Some Biochemical Parameters and Brain Oxidative Stress in Experimental Rats Exposed Chronically to Silver Nitrate and the Protective Role of Vitamin E and Selenium. Toxicol. Res. 2016;32(4): 301-309. doi:10.5487/TR.2016.32.4.301
18- Buege JA, Aust SD. Microsomal lipid peroxidation. Methods Enzymol. 1978; 52:302–310. doi: 10.1016/s0076-6879 (78)52032-6.
19- Sastry KV, Moudgal RP, Mohan J, Tyagi JS, Rao GS. Spectrophotometric determination of serum nitrite and nitrate by copper-cadmium alloy. Anal Biochem. 2002;306(1):79-82. doi:10.1006/abio.2002.5676.
20- VanGuilder HD, Vrana KE, Freeman WM. Twenty-five years of quantitative PCR for gene expression analysis, Biotechniques. 2008; 44:619–626. https://doi.org/10.2144/000112776
21- Suvarna K S, Layton A C, Bancroft J D. Bancroft's Theory and Practice of Histological Techniques E-Book, Elsevier Health Sciences. 2018.
22- Drury R. & Wallington E. Carleton's Histological Techniques (6thedn.) Oxford University Press. New York, Toronto, USA. 1980.
23- Elbassuoni EA, Abdel Hafez SM. Impact of chronic exercise on counteracting chronic stress-induced functional and morphological pancreatic changes in male albino rats. Cell Stress Chaperones. 2019;24(3):567-580. doi:10.1007/s12192-019-00988-y
24- Cote S. Current protocol for light microscopy immunocytochemistry. Immunohistochemistry, II, 1993, 148-167.
25- Abdel Hafez SMN. Age related changes in the dermal mast cells and the associated changes in the dermal collagen and cells: A histological and electron microscopy study. Acta Histochem. 2019;121(5):619-627. doi:10.1016/j.acthis.2019.05.004.
26- van der Zande M, Vandebriel RJ, Van Doren E, et al., Distribution, elimination, and toxicity of silver nanoparticles and silver ions in rats after 28-day oral exposure. ACS Nano. 2012;6(8):7427-7442. doi:10.1021/nn302649p
27- Tiwari R, Singh RD, Binwal M, et al., Perinatal exposure to silver nanoparticles reprograms immunometabolism and promotes pancreatic beta-cell death and kidney damage in mice. Nanotoxicology. 2021;15(5):636-660. doi:10.1080/17435390.2021.1909767
28- Salem F, Lokman R, Kassab R. Ameliorative eff ects of wateryextracts of boswella serrata and syzygium aromaticum on L-arginine induced acute pancreatitis in rats, World J. Pharm. Res. 3 (2014) 71–87.
29- Abdelzaher WY, Ahmed SM, Welson NN, Marraiki N, Batiha GE, Kamel MY. Vinpocetine ameliorates L-arginine induced acute pancreatitis via Sirt1/Nrf2/TNF pathway and inhibition of oxidative stress, inflammation, and apoptosis. Biomed Pharmacother. 2021; 133:110976. doi:10.1016/j.biopha.2020.110976
30- Tsai TH, Lin CJ, Chua S, et al. Melatonin attenuated the brain damage and cognitive impairment partially through MT2 melatonin receptor in mice with chronic cerebral hypoperfusion [published correction appears in Oncotarget. 2020 Sep 22;11(38):3558]. Oncotarget. 2017;8(43):74320-74330. Published 2017 Aug 22. doi:10.18632/ oncotarget. 20382.
31- Abdelzaher WY, Rofaeil RR, Ali DME, Attya ME. Protective effect of dipeptidyl

peptidase-4 inhibitors in testicular torsion/detorsion in rats: a possible role of HIF-1α and nitric oxide. Naunyn Schmiedebergs Arch Pharmacol. 2020; 393(4):603-614. doi:10.1007/s00210-019-01765-5

32- Rofaeil RR, Ahmed SM, Bahaa HA, Mahran A, Welson NN, Abdelzaher WY. Dipeptidyl peptidase-4 inhibitor: Sitagliptin down-regulated toll-like receptor 4 signaling pathway to reduce uterine injury in rats. Iran J Basic Med Sci. 2022;25(11):1396-1401. doi:10.22038/IJBMS.2022.64552.14202

33- Kong L, Deng J, Zhou X, et al., Sitagliptin activates the p62-Keap1-Nrf2 signalling pathway to alleviate oxidative stress and excessive autophagy in severe acute pancreatitis-related acute lung injury. Cell Death Dis. 2021;12(10):928. Published 2021 Oct 11. doi:10.1038/s41419-021-04227-0

34- Abdel-Hakeem EA, Abdel-Hamid HA, Abdel Hafez SMN. The possible protective effect of Nano-Selenium on the endocrine and exocrine pancreatic functions in a rat model of acute pancreatitis. J Trace Elem Med Biol. 2020; 60:126480. doi:10.1016/j.jtemb.2020.126480

35- Mohamed MZ, Mohammed HH, Khalaf HM. Therapeutic effect of rupatadine against l-arginine-induced acute pancreastitis in rats: role of inflammation. Can J Physiol Pharmacol. 2022;100(2):176-183. doi:10.1139/cjpp-2021-0330.

36- Wadie W, Ahmed GS, Shafik AN, El-Sayed M. Effects of insulin and sitagliptin on early cardiac dysfunction in diabetic rats. Life Sci. 2022;299:120542. doi:10.1016/j.lfs.2022.120542.

37- Alnemri ES, Livingston DJ, Nicholson DW, Salvesen G, Thornberry NA, Wong WW, Yuan J. Human ICE/CED-3 protease nomenclature. Cell. 1996; 87:171. doi: 10.1016/S0092-8674(00) 81334-3.

38- Perry DK, Smyth MJ, Stennicke HR, Salvesen GS, Duriez P, Poirier GG, et al. Zinc is a potent inhibitor of the apoptotic protease, caspase-3. A novel target for zinc in the inhibition of apoptosis. J Biol Chem. 1997;272:18530–18533. doi: 10.1074/jbc.272.30.18530.

39- Kolesarova A, Capcarova M, Sirotkin AV, Medvedova M, Kovacik J. In vitro assessment of silver effect on porcine ovarian granulosa cells. J Trace Elem Med Bio. 2011; 25:166–170. doi: 10.1016/j.jtemb.2011.05.002

40- Eom HJ, Ahn JM, Kim Y, Choi J. Hypoxia inducible factor-1 (HIF-1)-flavin containing monooxygenase-2 (FMO-2) signaling acts in silver nanoparticles and silver ion toxicity in the nematode, Caenorhabditis elegans. Toxicol Appl Pharmacol. 2013;270(2): 106-113. doi:10.1016/j.taap.2013.03.028

41- Wang X, Li J, Wu D, Bu X, Qiao Y. Hypoxia promotes apoptosis of neuronal cells through hypoxia-inducible factor-1α-micro RNA-204-B-cell lymphoma-2 pathway. Exp Biol Med (Maywood). 2016; 241(2):177-183. doi:10.1177/1535370215600548.

42- Kowalski E, Geng S, Rathes A, Lu R, Li L. Toll-interacting protein differentially modulates HIF1α and STAT5-mediated genes in fibroblasts. J Biol Chem. 2018;293(31):12239-12247. doi:10.1074/jbc.RA118.003382

43- Puri S, Cano DA, Hebrok M. A role for von Hippel-Lindau protein in pancreatic beta-cell function. Diabetes. 2009;58(2): 433-441. doi:10.2337/db08-0749.

44- Jiang BH, Semenza GL, Bauer C, Marti HH. Hypoxia-inducible factor 1 levels vary exponentially over a physiologically relevant range of O2 tension. Am J Physiol. 1996; 271(4 Pt 1): C1172-C1180. doi:10.1152/ajpcell.1996.271.4.C1172.

45- Qin G, Tang S, Li S, et al., Toxicological evaluation of silver nanoparticles and silver nitrate in rats following 28 days of repeated oral exposure. Environ Toxicol. 2017;32(2):609-618. doi:10.1002/tox.22263

46- Steinel NC, Bolnick DI. Melanomacrophage Centers As a Histological Indicator of Immune Function in Fish and Other Poikilotherms. Front Immunol. 2017; 8: 827. Published 2017 Jul 17. doi:10.3389/fimmu.2017.00827

47- Okuno M, Minami K, Okumachi A, et al., Generation of insulin-secreting cells from pancreatic acinar cells of animal models of type 1 diabetes. Am J Physiol Endocrinol Metab. 2007;292(1):E158-E165. doi:10.1152/ajpendo.00180.2006.